Indomethacin-induced oxidative stress enhances death receptor 5 signaling and sensitizes tumor cells to adoptive T-cell therapy

Nada S Aboelella ![ORCID],[1] Caitlin Brandle,[1] Ogacheko Okoko,[1] Md Yeashin Gazi,[1] Zhi-Chun Ding,[1] Hongyan Xu,[2] Gregory Gorman ![ORCID],[3] Roni Bollag,[1,4] Marco L Davila ![ORCID],[5] Locke J Bryan,[1,6] David H Munn,[1,7] Gary A Piazza,[8] Gang Zhou ![ORCID] [1,6]

Correspondence to
Dr Gang Zhou;
gzhou@augusta.edu

ABSTRACT

Background Adoptive cell therapy (ACT) using genetically modified T cells has evolved into a promising treatment option for patients with cancer. However, even for the best-studied and clinically validated CD19-targeted chimeric antigen receptor (CAR) T-cell therapy, many patients face the challenge of lack of response or occurrence of relapse. There is increasing need to improve the efficacy of ACT so that durable, curative outcomes can be achieved in a broad patient population.

Methods Here, we investigated the impact of indomethacin (indo), a non-steroidal anti-inflammatory drug (NSAID), on the efficacy of ACT in multiple preclinical models. Mice with established B-cell lymphoma received various combinations of preconditioning chemotherapy, infusion of suboptimal dose of tumor-reactive T cells, and indo administration. Donor T cells used in the ACT models included CD4$^+$ T cells expressing a tumor-specific T cell receptor (TCR) and T cells engineered to express CD19CAR. Mice were monitored for tumor growth and survival. The effects of indo on donor T cell phenotype and function were evaluated. The molecular mechanisms by which indo may influence the outcome of ACT were investigated.

Results ACT coupled with indo administration led to improved tumor growth control and prolonged mouse survival. Indo did not affect the activation status and tumor infiltration of the donor T cells. Moreover, the beneficial effect of indo in ACT did not rely on its inhibitory effect on the immunosuppressive cyclooxygenase 2 (COX2)/prostaglandin E2 (PGE2) axis. Instead, indo-induced oxidative stress boosted the expression of death receptor 5 (DR5) in tumor cells, rendering them susceptible to donor T cells expressing TNF-related apoptosis-inducing ligand (TRAIL). Furthermore, the ACT-potentiating effect of indo was diminished against DR5-deficient tumors, but was amplified by donor T cells engineered to overexpress TRAIL.

Conclusion Our results demonstrate that the pro-oxidative property of indo can be exploited to enhance death receptor signaling in cancer cells, providing rationale for combining indo with genetically modified T cells to intensify tumor cell killing through the TRAIL-DR5 axis. These findings implicate indo administration,

WHAT IS ALREADY KNOWN ON THIS TOPIC

⇒ The increased basal level of oxidative stress in cancer cells renders them more susceptible to redox disruption. It is well-documented that non-steroidal anti-inflammatory drugs (NSAIDs) can induce oxidative stress in cancer cells and cause growth inhibition. Emerging evidence indicates that induction of oxidative stress in cancer cells by tumor-reactive T cells contributes to the efficacy of adoptive T cell therapy (ACT). Whether the pro-oxidative activity of NSAIDs can augment the efficacy of ACT has not been explored.

WHAT THIS STUDY ADDS

⇒ We demonstrate that administration of indomethacin potentiates ACT in multiple preclinical models. Mechanistically, indomethacin-induced oxidative stress leads to enhanced expression of death receptor 5 (DR5) in cancer cells, sensitizing cancer cells to the cytotoxicity of tumor-reactive T cells through the TRAIL-DR5 axis.

HOW THIS STUDY MIGHT AFFECT RESEARCH, PRACTICE OR POLICY

⇒ Administration of indomethacin, and potentially other NSAIDs, represents a readily applicable and cost-effective approach to improve the therapeutic outcome of ACT.

and potentially similar use of other NSAIDs, as a readily applicable and cost-effective approach to augment the efficacy of ACT.

INTRODUCTION

Adoptive cell therapy (ACT) using T cell infusion products genetically modified to express tumor-specific TCRs or CARs has resulted in remarkable therapeutic outcomes in some patients with certain types of malignancies.[1 2] However, the therapeutic potential of ACT as a treatment modality for various types

of cancer in a broad patient population has yet to be fulfilled.[3 4] Even for CD19-targeted CAR T cell therapy, the most advanced and clinically validated ACT, many patients failed to respond to therapy or succumbed to post-therapy relapse.[5] Thus, finding ways to improve the efficacy of ACT has the potential to deliver durable, curative therapeutic benefits to more patients.

Cancer cells are often under a higher degree of basal level oxidative stress than normal cells, as reflected by increased presence of reactive oxygen species (ROS), likely driven by cell-intrinsic transformation events such as oncogene activation, tumor suppressor gene inactivation and altered metabolism, or by exogenous insults such as irradiation and chemotherapy.[6 7] As a result, cancer cells tend to have increased dependence on the endogenous antioxidant defense systems to maintain redox homeostasis, making them more vulnerable than normal cells to further redox disruptions. The idea of targeting tumor redox homeostasis to achieve selective tumor killing has led to the development of numerous pro-oxidants that can incite oxidative stress in cancer cells either by promoting ROS production or by inhibiting the antioxidant systems.[8–12] However, application of pro-oxidants as monotherapy for cancer has encountered challenges including inefficient drug delivery, lack of drug stability, limited tumor specificity, and tumor heterogeneity.

We recently reported that ACT can profoundly alter tumor redox metabolism, resulting in increased ROS accumulation and oxidative DNA damage in cancer cells.[13] These results suggest that tilting tumor redox balance toward oxidative destruction is critical for the efficacy of ACT, raising the possibility that pro-oxidants can be employed to intensify tumor oxidative stress so as to sensitize tumor cells to ACT. Non-steroidal anti-inflammatory drugs (NSAIDs), which are widely used for pain relief and reducing inflammation, are known to induce oxidative and endoplasmic reticulum (ER) stresses that cause cancer cell apoptosis.[14–22] Meanwhile, it has been well established that NSAIDs can exert antitumor effects by inhibiting the tumor-promoting COX/PGE2 axis. Inhibition of PGE2 can also mitigate immunosuppression in the tumor microenvironment (TME), leading to improved antitumor immunity.[23 24] In this regard, compelling evidence from preclinical studies indicates that certain NSAIDs can augment the efficacy of anti-PD1 therapy,[25 26] propelling the interest of applying NSAIDs to potentiate immune checkpoint blockade therapy. Although it has been reported that NSAIDs can sensitize tumor cells to CD19CAR T cell cytotoxicity in vitro,[27] in vivo evidence supporting the use of NSAIDs in the setting of ACT is still lacking.

In this study, we set out to examine how administration of indomethacin (indo), a commonly used NSAID, shapes the therapeutic outcome of ACT in model systems where tumor-specific CD4$^+$ T cells or CD19CAR T cells are used to treat murine or human B-cell lymphomas. Our results reveal oxidative stress-induced tumor-intrinsic death receptor signaling as the molecular basis by which indo potentiates the antitumor efficacy of tumor-reactive T cells, supporting repurposing NSAIDs for cancer treatment in the context of T cell adoptive immunotherapy.

METHODS

Cell lines and cell culture conditions

A20 and CT26 tumor cell lines were purchased from the American Type Culture Collection. The generation of A20 cells expressing influenza hemagglutinin (A20HA) was described elsewhere.[28] The death receptor 5 knockout A20 cell line (A20.DR5 KO) was generated using the Alt-R CRISPR-Cas9 System (IDT) following the manufacturer's instruction. Limiting dilution was performed and single cell clones were analyzed by flow cytometry to select for DR5-negative clones. Nucleotide deletion in the targeted *Dr5* gene loci was confirmed by DNA sequencing. A20.luciferase cells (A20.Luci) were generated by transducing A20 cells with retroviruses carrying luciferase (MSCV-luciferase). Murine CD19-expressing CT26 tumor cell line (CT26.mCD19) was created by transducing CT26 cells with a vector carrying murine CD19 (MSCV-mCD19). CD19$^+$ tumor cells were subsequently FACS-sorted and expanded. Human B-cell lymphoma cell line Raji was provided by Dr. Huidong Shi (Augusta University). Human colorectal carcinoma cell line HT29 was provided by Dr. Gary A. Piazza (Auburn University). All tumor cell lines were cultured in RPMI 1640 (HyClone Laboratories) culture medium supplemented with 10% fetal bovine serum albumin (FBS), 1% penicillin/streptomycin (HyClone Laboratories), 1% non-essential amino acids, 1% glutamine and 0.1mM 2-mercaptoethanol at 37°C in a 5% CO2 incubator.

Experimental mice

BALB/c mice (5–8 weeks old) were purchased from Charles River NCI at Frederick. TCR-Tg (6.5) mice on a BALB/c (Thy1.1) background expressing an αβTCR specific for amino acids 110–120 from influenza HA presented by MHC class II molecule IE^d were described previously.[29] BALB/c mice on the CD45.1 background and immunodeficient nonobese diabetic (NOD)–severe combined immunodeficient (Scid) IL-2Rγ-null (NSG) mice were purchased from the Jackson Laboratory. All mice were housed under specific pathogen-free conditions by Laboratory Animal Services of the Augusta University.

Mouse and human T cell viral transduction

The retroviral vector MSGV-1D3-28Z.1–3 containing mouse CD19-targeting CAR (mCD19CAR) was provided by James N. Kochenderfer at National Cancer Institute.[30] The retroviral vector MSCV-luciferase was generated as described previously.[31] The retroviral vector MSCV-mTnfsf10 containing mouse TRAIL was purchased from VectorBuilder. The retroviral vector SFG-humCD1928z containing human CD19-targeting CAR (hCD19CAR) was described elsewhere.[32] Retroviral supernatants

preparation and murine T cell retroviral transduction procedures were described previously.[31] Phoenix Amphotropic cells were transfected with hCD19CAR retroviral vector using Lipofectamine 2000 to produce viral supernatants. Human T cells were isolated from the buffy coat of healthy donors using the EasySep Human T Cell Isolation Kit (STEMCELL Technologies). Purified T cells were activated by T-Activator CD3/CD28 Dynabeads (ThermoFisher) in the presence of hIL-2 (30 U/mL) for 48 hours. Activated T cells were spin-infected twice on two consecutive days with hCD19CAR retroviral supernatant using retronectin. Human T cells were further expanded for 7 days in the presence of hIL-2 (100 U/mL) before harvest for adoptive transfer.

Animal tumor models and in vivo treatments

Tumor cells were subcutaneously injected to the right flank of mice. The following numbers of tumor cells in 100 µl volume were used for each mouse: 5×10^6 for murine B-cell lymphoma cells (A20HA, A20 and A20.DR5KO), 3×10^6 for human B-cell lymphoma Raji cells, and 1×10^6 for murine colon cancer CT26.mCD19 cells. Tumor growth was monitored by caliper measurement every other day. Tumor areas were calculated as the product of two perpendicular diameters in square millimeters (mm^2). When tumor sizes reached the desired sizes as indicated in specified experiments, mice were randomly assigned into groups to receive the specified treatments. CTX was injected intraperitoneally to mice at 150 mg/kg 1 day before T cell transfer. Indo was intraperitoneally injected to mice at 1 mg/kg. Indo administration started 4 hours before T cell transfer and continued daily for 28 days. Mice were euthanized when tumor sizes reached $300\,mm^2$. For T cell transfer using unstimulated HA-specific $CD4^+$ T cells, spleens collected from 6.5-Tg Thy1.1$^+$ mice were processed into single cell suspensions. $\sim 5 \times 10^6$ HA-specific $CD4^+$ T cells were injected to each mouse via tail vein. For T cell transfer using pre-activated HA-specific $CD4^+$ T cells, $CD4^+$ T cells were isolated from the spleens of from 6.5-Tg mice using an EasySep Mouse $CD4^+$ T Cell Isolation Kit (STEMCELL Technologies). Isolated $CD4^+$ T cells were activated and expanded in vitro with T-Activator CD3/CD28 Dynabeads (ThermoFisher) for 3 days. 1.0×10^5 activated HA-specific $CD4^+$ T cells were injected to mice via tail vein. For CAR T cell transfer, $\sim 3 \times 10^6$ mCD19CAR$^+$ or $\sim 0.8 \times 10^6$ hCD19CAR$^+$ T cells were transferred to each mouse.

Antibodies and reagents

Single cell suspensions were stained for flow cytometry analysis using the following fluorochrome-conjugated antibodies specific to murine CD4 (GK1.5), CD8 (53–6.7), CD90.1 (OX-7), CD45R/ B220 (RA3-6B2), CD19 (6D5), CD262 (DR5) (MD5-1), CD253 (TRAIL) (N2B2), CD44 (IM7), CD62L (MEL-14), PD1 (RMP1-14), CD11b (M1/70), CD45.1 (A20), CD45.2 (104), anti–IL-2 (JES6-5H4), anti–TNF-α (MP6-XT22), anti–IFN-γ (XMG1.2), anti–GM-CSF (MP1-22E9), anti-GzmB (GB11), and antibodies specific to human CD4 (OKT4), CD8a (HIT8a) and CD262 (DR5) (DJR2-4). Antibodies were purchased from Biolegend unless otherwise noted. Anti-mouse FOXP3 (FJK-16s), and BCL-2 (Bcl2/100) were purchased from eBioscience. MCL-1 (B-6) (sc-74436) and Anti-FLIPS/L Antibody (G-11) (sc-5276) were purchased from Santa Cruz Biotechnology. Anti-COX2 (#10010096) antibody was purchased from Cayman Chemical. Polyclonal mouse anti-rat F(ab')2 antibody and isotype control antibody were purchased from Jackson Immuno Research. Cyclophosphamide (CTX) was purchased from Tokyo Chemical Industry (Tokyo, Japan). Indomethacin was purchased from Sigma-Aldrich. N-Acetyl-L-cysteine was purchased from Alfa Aesar. DR5 agonist antibody (MD5-1) was purchased from Bio X cell. Lipofectamine 2000 was purchased from ThermoFisher Scientific. Retronectin was purchased from Takara. D-Luciferin monosodium salt was purchased from Pierce.

Sample preparation and flow cytometry analysis

Spleen and tumor samples were processed into single-cell suspensions. For surface molecule detection, cells were stained with fluorochrome-conjugated antibodies for 15 min at room temperature in the dark. To detect intracellular molecules, including cFLIP, MCL-1, BCL2, COX2, and FOXP3, cells were stained with surface markers followed by intracellular staining using the Foxp3 Transcription Factor Staining Buffer Set (eBioscience). For cytokine intracellular staining, T cells in splenocytes or tumor cell suspensions were stimulated with the GolgiPlug Leukocyte Activation Cocktail (BD Biosciences) for 3.5 hours at 37°C. Cells were harvested and surface stained, followed by cytokine staining using the Fixation/Permeabilization Solution Kit (BD Biosciences). For detection of mCD19CAR expression in transduced murine T cells, polyclonal mouse anti-rat-F(ab')2 antibody was used to detect 1D3 scFv with normal polyclonal mouse IgG antibody as the isotype control. For detection of hCD19CAR expression in transduced human T cells, biotinylated L protein was used to stain cells followed by PE-conjugated streptavidin (SA) as described previously.[33] For intracellular ROS measurement, ROS was detected using the cell permeant CM-H2DCFDA (ThermoFisher) as previously described.[13] To evaluate tumor cell death triggered by DR5 signaling, 96-well protein A-coated plates (Pierce) were used to coat MD5-1, a DR5 agonist antibody, as previously described.[34] In brief, wells in a protein A-coated plate were coated with 50 µL phosphate-buffered saline (PBS) or purified MD5-1 antibody (10 mg/mL) at 4°C overnight and washed with PBS before use. 1.0×10^5 A20 or A20.DR5KO cells were seeded into each well in 200 µL culture media not containing 2-mercaptoethanol. DMSO or indomethacin was added to PBS or MD5-1-coated wells as indicated. After overnight culture at 37°C, cells were harvested for Annexin V staining (BioLegend) following manufacturer's instruction. DAPI (0.5 µg/mL) was added to cells before flow cytometry analysis.

Bioluminescent imaging

Bioluminescent imaging (BLI) was performed on a Spectral Advanced Molecular Imaging X (Ami X) system (Spectral Instruments Imaging) to detect tumor-infiltrating donor T cells as we previously described.[35] Briefly, luciferase-carrying viruses were used to transduce donor T cells.

Luciferase-labeled HA-specific CD4^{+} T cells or mCD19CAR T cells were used for adoptive transfer. For imaging, each mouse received an intraperitoneal injection of 150 mg/kg luciferin and was anesthetized by inhalation of 2% isoflurane. The photographic images were acquired and overlaid with pseudocolor luminescent images. All BLI data were analyzed using the Aura Imaging Software (Spectral Instruments Imaging). The luminescence signal in the tumor region was quantified as photon/sec as an indicator of the density of donor T cells in tumor.

RNA extraction and quantitative real-time PCR

Tumor cells were harvested after overnight treatment under the indicated conditions. RNA was extracted using TRIZOL Reagent (ThermoFisher Scientific). 1 µg of RNA was used to generate cDNA using the SuperScript III First-Strand Synthesis System (ThermoFisher Scientific). Quantitative real-time PCR was performed using SYBR Green Mix (Bio-Rad) on a BioRad iCycler equipped with an iCycler iQ Detection System. β-actin was used to normalize target gene RNA expression levels. Each sample was assayed in triplicates. All primers were purchased from Integrated DNA Technologies. The sequences of the PCR primers are shown in online supplemental table 1.

Detection of prostaglandin E2 (PGE2) and indomethacin

To quantify the levels of PGE2 and indomethacin in tumor tissues, mice were sacrificed, and tumors were excised, weighed and cryopreserved in −80°C. Tumor samples and controls were homogenized 1:10 with 5 mM ammonium acetate buffer using an Omni THQ homogenizer. Due to the endogenous amount of PGE2 in the tumor, calibration standards, blanks and QCs were prepared by spiking 5 mM ammonium acetate (50 µL) with the appropriate amount of PGE2 and indomethacin to achieve concentrations ranging from 0.5 to 10,000 ng/mL. Blank and QC samples were also prepared in tumor homogenate for each analyte. Standards, blanks, QCs and samples were spiked with internal standard (10 µL of 1000 ng/mL PGE2 and indomethacin in acetonitrile). Acetonitrile (500 µL) was added to an equal sample volume of tumor homogenate to precipitate the proteins and vortexed well. After centrifugation for 5 min at $21\,000 \times g$, the supernatant was transferred to an autosampler vials and analyzed by liquid chromatography–mass spectrometry (LC/MS/MS). The LC/MS/MS system consisted of Shimadzu system (Columbia MD) equipped with LC20-AD dual HLPC pumps, an SIL20-AC HT autosampler, and a DGU-20A2 in-line degasser. Detection was performed using an Applied BioSystems 5500 QTRAP (Applied Biosystems, Foster City, CA) triple quadrupole mass spectrometer operated in the positive ion mode. Mass calibration, data acquisition and quantitation were performed using Applied Biosystem Analyst V.1.7.2 software (Applied Biosystems, Foster City, California, USA).

Statistical analysis

Data were analyzed using Prism V.8.0 (GraphPad Software). Experimental values are expressed as mean±SE of mean (SEM). Survival was compared using a Log-rank (Mantel-Cox) test. For comparison between two groups, statistical analysis was performed using unpaired Student's t-test. One-way analysis of variance followed by Tukey's multiple testing correction was used for comparison of more than two groups. P values less than 0.05 were considered statistically significant.

RESULTS

Indo enhances the efficacy of ACT in a mouse B-cell lymphoma model

Initial experiments were conducted to determine if indo administration could enhance the efficacy of ACT in a well-characterized murine B-cell lymphoma model system.[28 29 31] In this system, mice with established A20 tumors expressing a model tumor antigen HA (A20HA) received pre-conditioning chemotherapy with cyclophosphamide (CTX), followed by infusion of splenocytes containing HA-specific CD4^{+} T cells (HA-CD4$_{sp}$) derived from 6.5 TCR-Tg mice (figure 1A). Indo was administered daily for 28 days by intraperitoneal injection at a dose of 1 mg/kg. Indo alone did not have any discernable impact on tumor growth compared with untreated mice (figure 1A,B, indo vs noTx). CTX alone transiently delayed tumor growth and moderately improved survival, but all mice succumbed to relapse. Indo administration following CTX (CTX+indo) did not improve tumor growth control or mouse survival compared with the CTX only group. Tumor growth inhibition was observed when CTX-conditioned mice were infused with HA-CD4^{+} T cell-containing splenocytes (CTX+HA-CD4$_{sp}$), in which 20% of mice in this treatment group achieved complete tumor regression. Notably, indo administration in addition to splenocyte infusion (CTX+HA-CD4$_{sp}$+indo) further improved tumor growth inhibition and led to complete tumor regression in 60% of mice. Lowering the indo dose to 0.3 mg/kg resulted in loss of the beneficial effect, and increasing the dose to 4 mg/kg resulted in toxicity in mice as reflected by severe weight loss (data not shown). Thereafter we used indo at 1 mg/kg dose for all in vivo studies.

Clinical application of ACT often involves reiterated stimulation of patient-derived T lymphocytes to expand and/or genetically modify them to generate the final infusion products. To model this scenario in mice, CD4^{+} T cells isolated from the splenocytes of TCR-Tg mice were expanded ex vivo with CD3/CD28 T-Activator Dynabeads. We performed a cell number titration experiment and found that adoptive transfer of 0.1 million activated HA-CD4^{+} T cells (HA-CD4$_{act}$) to CTX-conditioned tumor-bearing mice resulted in significant tumor growth delay, but only occasional complete tumor regression. We used this suboptimal therapeutic condition in subsequent experiments to examine the impact of indo administration on ACT efficacy. Consistent with the results of ACT using TCR-Tg splenocytes, indo administration following adoptive transfer of activated HA-specific CD4^{+} T cells
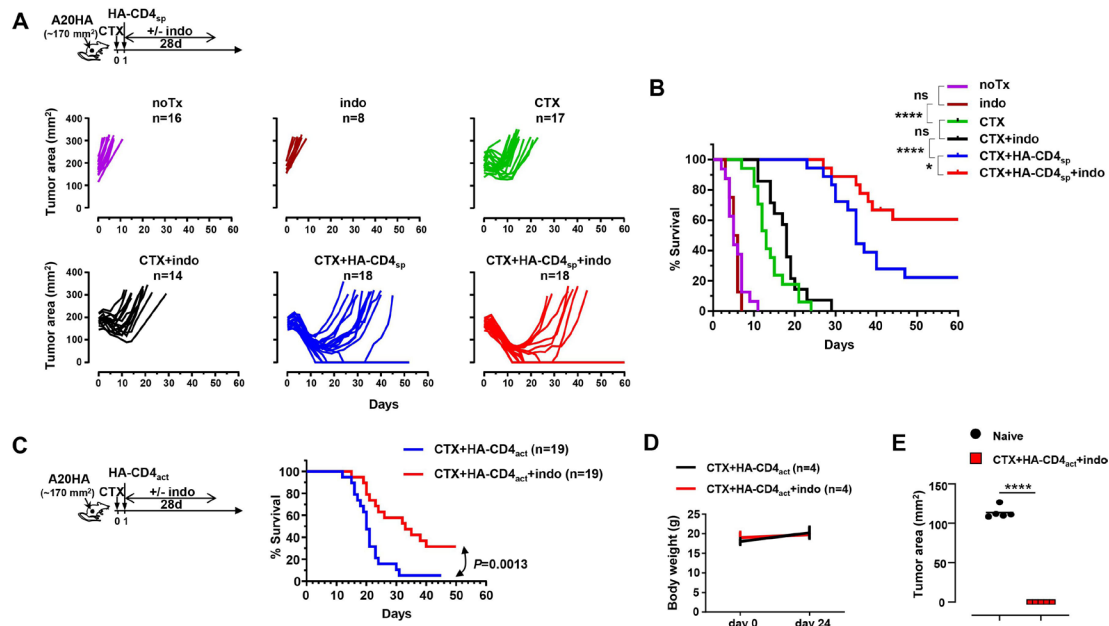
Figure 1 Indomethacin administration in an ACT setting enhances the antitumor effects of tumor-specific CD4+ T cells against established B-cell lymphoma. (A) Indo enhances the efficacy of ACT using unstimulated HA-specific CD4+ T cells. The schema demonstrates the timeline of experimental procedures. When tumor sizes reached ~170 mm², mice were randomly divided into groups to receive the indicated treatment conditions. CTX was given to mice via i.p. injection at 150 mg/kg. Indo was administered to mice daily at 1 mg/kg for 28 days, starting 4 hours before T cell transfer. Splenocytes from 6.5-Tg Thy1.1 mice containing unstimulated HA-specific CD4+ T cells were transferred to mice via tail vein. The results of three independent experiments are pooled for analysis. Tumor growth curves of individual mice in each group are shown. The number of mice in each group is given. Mouse survival is summarized in the Kaplan-Meier plot (B). (C) Indo improves the efficacy of ACT using preactivated tumor-specific CD4+ T cells. Following the experimental timeline depicted in the schema, mice with established A20HA tumors received CTX conditioning followed by adoptive transfer of CD3/CD28 Dynabead-activated HA-specific CD4+ T cells. One group of mice was administered indo for 28 days, starting on the day of T cell transfer. The results of three independent experiments are pooled for analysis. Mouse survival is summarized in the Kaplan-Meier plot. The number of mice in each group is given. (D) Mouse weight changes before and after treatment in one representative experiment. (E) Mice with complete tumor regression are resistant to tumor rechallenge. Mice that had undergone complete tumor regression after receiving CTX+HA-CD4$_{act}$.+indo were rechallenged with 5×10⁶ A20HA tumor cells injected s.c. in the left flank (opposite to the original tumor side). Naïve mice injected s.c. with A20HA tumor cells were used as the control. Statistics: (B, C) Log-rank (Mantel-Cox) test, (D,E) Unpaired t-test. *P<0.05, ****p<0.0001, ns: non-significant. ACT, adoptive cell therapy.

(CTX+HA-CD4$_{act}$+indo) exhibited augmented antitumor activity, as reflected by significantly improved tumor growth inhibition and prolonged survival (figure 1C). It is noteworthy that indo administration at 1 mg/kg for 4 weeks did not cause weight loss in mice (figure 1D), indicating that treatment was well-tolerated at this dose. Moreover, the mice that had achieved complete tumor regression in the CTX+HA-CD4$_{act}$+indo group were resistant to tumor rechallenge (figure 1E), suggesting the formation of immune memory.

Indo enhances the efficacy of CD19CAR T cell therapy in murine and human B-cell lymphoma models

We next determined if the beneficial effect of indo could be replicated in more clinically relevant CD19CAR T cell therapy models. Mouse total T cells were transduced to express CAR targeting murine CD19 (mCD19CART) (figure 2A). In vitro killing assays showed that indo pretreatment rendered A20 B-cell lymphoma cells more sensitive to the cytotoxicity of mCD19CAR T cells (figure 2B,C). To test if indo could augment the efficacy of

mCD19CART in vivo, syngeneic BALB/c mice with established A20 tumors were conditioned with CTX followed by infusion of mCD19CAR T cells in the absence or presence of indo administration (figure 2D). As shown in figure 2D,E, indo by itself had no effect on tumor growth kinetics (indo vs noTx), nor did it improve the transient antitumor effect of CTX (CTX +indo vs CTX). However, the addition of indo significantly enhanced the efficacy of mCD19CART therapy (CTX +mCD19CART+indo vs CTX +mCD19CART).

We also tested whether indo could improve the efficacy of human CD19CAR T cell therapy in a xenograft tumor model. Total T cells from the PBMC of healthy donors were transduced with a retroviral vector carrying human CD19-targeting CAR (hCD19CART) as previously reported.[32] The transduction efficiency of hCD19CAR T cells was 50%–60% (online supplemental figure 1A), and the reactivity of transduced T cells to CD19-expressing human B-cell lymphoma Raji cells was verified in vitro (online supplemental figure 1B). For in vivo studies, Raji
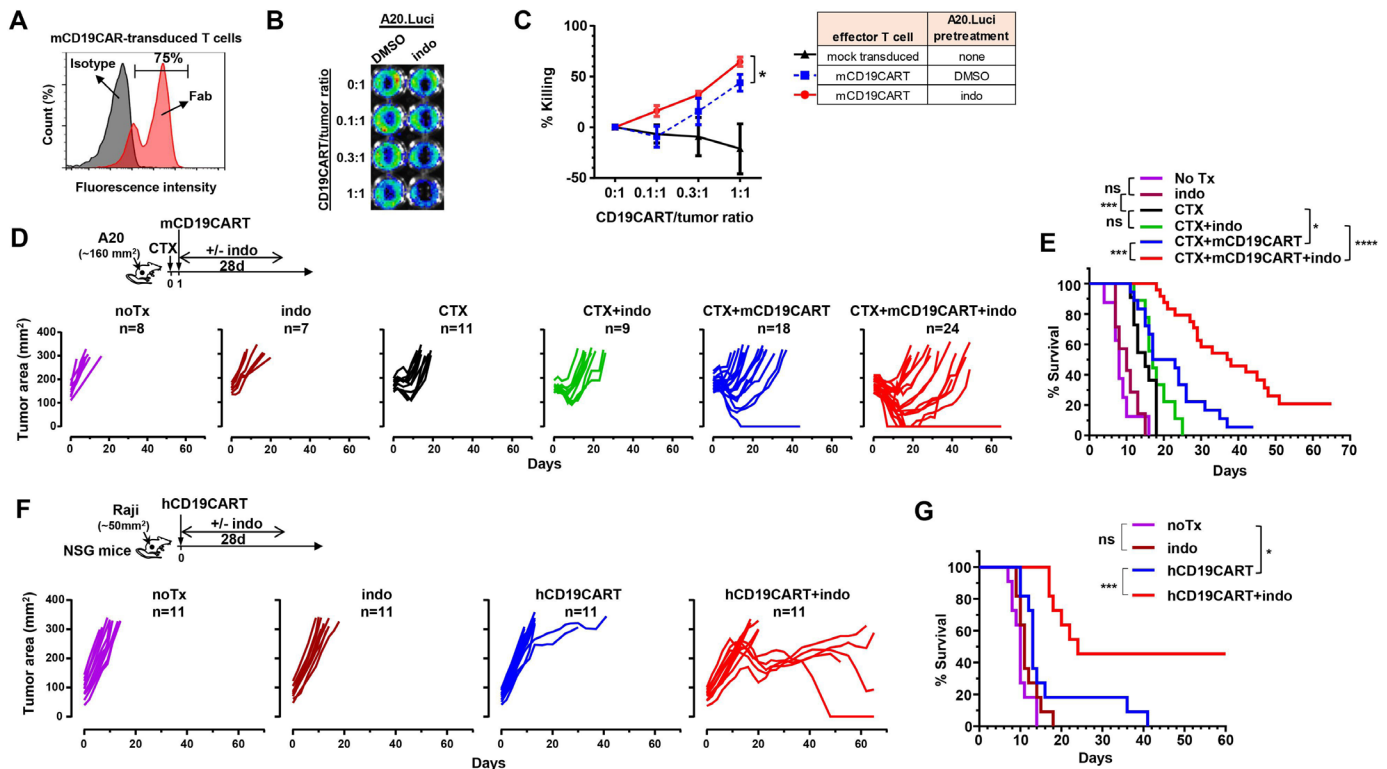
Figure 2 Indomethacin enhances the efficacy of CD19CART in both mouse and human B cell lymphoma models. (A) Generation of mCD19CAR T cells. Total T cells isolated from the splenocytes of CD45.1 mice were activated and transduced with 1D3-28Z.1–3-carrying retroviruses to express mCD19CAR. Mouse anti-rat-Fab Ab (Fab) was used to detect the 1D3 scFv to evaluate T cell transduction efficiency. Isotype antibody stain was used as the negative control. (B) BLI-based CD19CART in vitro tumor killing assay. 0.1 million CD19+ A20.Luci cells were seeded in the absence or presence of increasing amounts of CD19CART cells. After overnight culture, BLI was performed to record the bioluminescent photon intensity (PI) in each well, which correlates with the quantity of live tumor cells. (C) Indo sensitizes tumor cells to CD19CART cell killing. A20.Luci cells were treated with solvent DMSO or 20 µg/mL indo overnight. After thorough washing, 0.1 million A20.Luci cells were mixed with increasing doses of CD19CART cells. Untransduced T cells were used as controls. PI was recorded by BLI after overnight culture. Cytotoxicity of CD19CART cells on A20.Luci is reflected by percent killing calculated as per cent of ($PI_{(tumor\ alone)}$ – $PI_{(tumor+CD19CART)}$)/$PI_{(tumor\ alone)}$). (D) Indo enhances the efficacy of mCD19CART against A20 murine lymphoma in syngeneic mice. The schema depicts the timeline of experimental procedures. When tumor size reached ~150 mm², A20-bearing BALB/c mice were randomly divided into groups to receive the indicated treatments. The results of three independent experiments are pooled for analysis. Tumor growth curves of individual mice in each group are shown. The number of mice in each group is given. Mouse survival is summarized in the Kaplan-Meier plot (E). (F) Indo enhances the efficacy of hCD19CART against Raji human lymphoma in NSG mice. Following the experimental timeline depicted in the schema, NSG mice with established Raji tumors (~50 mm²) were randomly divided into groups to receive the indicated treatments. A suboptimal dose of hCD19CAR T cells (1.5×10⁶) were used for transfer. The results of two independent experiments are pooled for analysis. Tumor growth curves of individual mice in each group are shown. The number of mice in each group is given. Mouse survival is summarized in the Kaplan-Meier plot (G). Statistics: (C) One-way ANOVA followed by Tukey's multiple comparison test, (E, G) Log-rank (Mantel-Cox) test. *P<0.05, ***p<0.001, ****p<0.0001, ns: non-significant. ANOVA, analysis of variance.

cells were subcutaneously implanted in the right flank of immunodeficient NSG mice. As shown in figure 2F, mice with established Raji tumors were divided into four groups to receive the indicated treatments: no treatment (noTx), indo, hCD19CART, or hCD19CART+indo. Indo alone did not alter tumor growth, and infusion of hCD19CART at the dose we used (0.7–0.9×10⁶ CAR⁺ cells) had only modest antitumor effects; however, the combination of indo and hCD19CART markedly delayed tumor growth and improved mouse survival (figure 2F,G).

Although CD19CAR T cell therapy has become an effective treatment option for patients with B-cell malignancies, so far CAR T therapy has had limited success

in treating solid tumors. We, therefore, tested if indo could potentiate CAR T therapy in a typical solid tumor model. For this purpose, mouse colorectal cancer CT26 cells were engineered to express murine CD19 (CT26.mCD19) (online supplemental figure 2A). CT26.mCD19 cells were implanted subcutaneously to the flank of BALB/c mice. Mice with established tumors received CTX-conditioning followed by infusion of a suboptimal dose of mCD19CART cells, in the absence or presence of indo administration (online supplemental figure 2B). The combination of indo and mCD19CART markedly improved mouse survival compared with mCD19CART alone (online supplemental figure 2B). Taken together,

our results suggest that the beneficial effect of indo in ACT is not limited to the CD4$^+$ T cell-based ACT model system, but may have broad implications for ACT including the use of genetically modified CAR T cells.

The beneficial effect of indo on ACT is independent of its COX2/PGE2 inhibitory activity

We sought to identify the molecular mechanism underlying the beneficial effect of indo on ACT. Indo is a nonselective COX inhibitor capable of blocking the production of PGE2. PGE2 in the TME can act to suppress antitumor immunity, and promote tumor progression, metastasis and chemoresistance.[23 36] To test whether the beneficial effect of indo in ACT was due to its inhibition of the COX/PGE2 axis, we examined the intracellular level of COX2 in tumor cells by flow-cytometry analysis. Figure 3A shows that COX2 was barely detectable in A20 cells but highly expressed in CT26 cells. Correspondingly, PGE2 was marginally detected by ELISA in the supernatants from cultured A20 cells whereas it was abundant in CT26 cell culture supernatants (figure 3B). Our data showing that CT26 cells contain high levels of COX2 and PGE2 was in line with the findings of published studies,[25 37] validating the robustness of our assays. Considering that PGE2 can be derived from tumor cells as well as stromal cells, we designed an experiment to measure the levels of PGE2 in the whole tumor mass. Using the HA-CD4$_{act}$ ACT model system as shown in figure 1, tumors were collected from mice under the specified treatment conditions. PGE2 in tumor tissues was quantified by LC-MS/MS. Figure 3C shows that PGE2 levels were marginally detected (5–40 ng/g) in all A20HA tumor tissues regardless of the treatment. In contrast, CT26 tumor tissues contained high levels of PGE2 (17933±9152 ng/g). Moreover, indo administration markedly reduced PGE2 in CT26 tumor tissues (1216±494 ng/g), reflecting the biological activity of indo in vivo. The presence of indo in tumors from indo-treated mice was confirmed and quantified by LC-MS/MS (figure 3D).

The low levels of PGE2 in A20 tumors as measured by LC-MS/MS analysis was in conflict with our initial expectation that indo-mediated PGE2 reduction led to enhance antitumor immunity in the lymphoma ACT models. To examine the impact of indo on T cells, we transferred T cells to CTX-conditioned tumor-bearing mice with or without indo administration and collected tumor tissues for FACS analysis at the specified time point (figure 3E). In the HA-CD4$_{act}$ ACT model, the frequencies of tumor-infiltrating donor T cells, and the percent distribution of naïve (CD44$^-$CD62L^{high}), effector memory (CD44$^+$CD62L^{low}) and central memory (CD44$^+$CD62L$^+$) subsets within the donor population were similar between the two groups (figure 3F). No differences were observed in the levels of T cell exhaustion markers PD-1 and Tim3 (figure 3G). In addition, donor T cells under the two conditions were comparable in producing functional molecules including IFNg, TNFa, IL2, GMCSF and GZMB (figure 3H). Furthermore, the frequencies of

immunosuppressive cells, including Foxp3$^+$ Tregs (in both donor and host CD4$^+$ T cells) and CD11b$^+$Gr1$^+$ MDSCs, were also similar between the two conditions (figure 3I). Similar results were observed for mCD19CAR T cells used in the ACT model, with the exception that mCD19CAR T cells produced more IL2 and GMCSF when indo was given after CAR-T infusion, likely reflecting some inherent differences between CAR-transduced T cells and TCR-Tg T cells (online supplemental figure 3A). Consistent with the FACS analysis data, BLI-based T cell tracking experiments indicate that indo administration did not alter, that is, neither enhanced nor reduced, donor T cell tumor infiltration in this ACT model (figure 3J,K). Similar donor T cell tumor infiltration patterns were observed in the ACT model in which mCD19CART cells were used for adoptive transfer (online supplemental figure 3B,C).

Collectively, our data indicate that the beneficial effect of indo in potentiating ACT against B-cell lymphoma appears to be independent of its inhibitory effects on COX/PGE2, and that indo administration does not directly impact the expansion, migration, activation and function of the donor T cells.

Indo-induced oxidative stress upregulates DR5 expression in tumor cells in vitro

Many NSAIDs, including indo, can induce oxidative stress in cancer cells, leading to apoptosis.[17–22] We confirmed that indo can induce oxidative stress, as indicated by increased ROS levels, in cultured mouse A20 lymphoma cells in a dose-dependent manner (figure 4A). Similar results were obtained for the human lymphoma cell line Raji (figure 4B), as well as mouse (CT26) and human (HT29) colon cancer cell lines (online supplemental figure 4). As expected, adding the antioxidant N-acetylcysteine (NAC) to the cultures neutralized indo's ability to induce ROS (figure 4C). It has been reported that indo-induced oxidative stress in cancer cells can activate the cellular stress sensor C/EBP-homologous protein (CHOP), which upregulates DR5, sensitizing tumor cells to TRAIL-mediated cell death.[20] We also found that A20 cells treated with indo had increased levels of molecules associated with oxidative/ER stress, including phosphorylated eIF2a (P-eIF2a), ATF4 and CHOP (online supplemental figure 5A). DR5 was constitutively expressed in A20 cells (online supplemental figure 5B). Indo treatment increased *Dr5* transcripts, along with genes associated with oxidative/ER stress, including *Nrf2*, *Ho-1*, *Atf4* and *Chop* (online supplemental figure 5C). Correspondingly, DR5 protein was found to be upregulated in A20 cells by indo in a dose-dependent manner (figure 4D). Enhanced expression of DR5 by indo was also observed in Raji cells (figure 4E). Indo-induced DR5 upregulation in A20 cells was abolished by the addition of NAC (figure 4F), implying the critical role of oxidative stress in enhancing DR5 expression. In addition, we found that indo treatment reduced the levels of cFLIP,
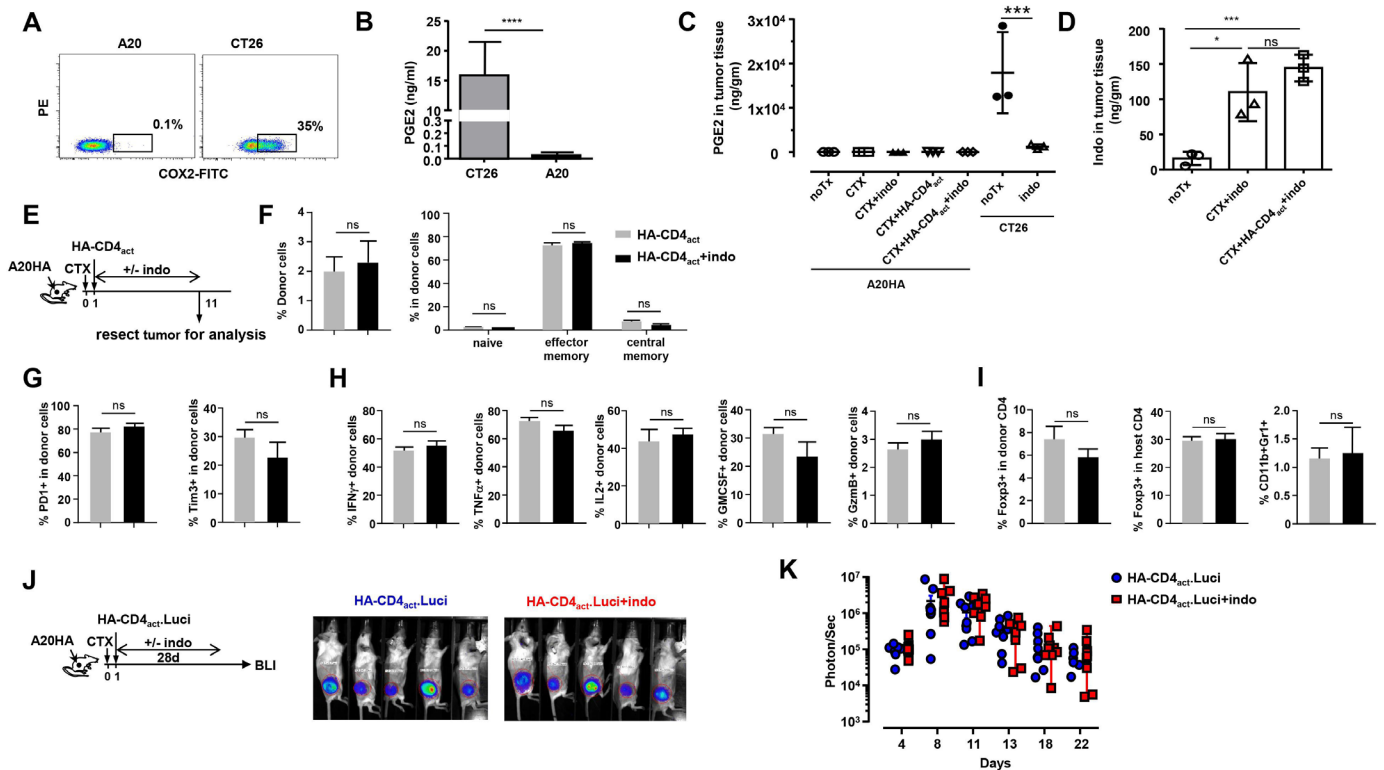
Figure 3 The beneficial effect of indo on ACT is independent of its COX2/PGE2 inhibitory activity and does not result in improved T cell phenotype. (A) A20 tumor cells express minimal levels of COX2. A20 tumor cells were cultured to confluence and then stained for intracellular COX2. CT26 cells, which are known to express COX2, were used as a positive control. Representative dot plots are shown. Numbers denote % of COX2-positive cells. (B) Paucity of PGE2 released by A20 cells. Grown to confluence, A20 and CT26 cell culture supernatants were collected for PGE2 measurement by ELISA. Each sample was measured in triplicate and results are shown as mean±SEM Data shown are representative of two independent experiments with similar results. (C) Measurement of PGE2 in tumor tissues by LC/MS. A20HA-bearing mice received the indicated treatments. Preactivated HA-specific CD4$^+$ T cells were used for adoptive transfer in this experiment following the procedure described in figure 1C. Ten days after T cell transfer, tumor tissues were collected from all mice and homogenized to measure PGE2. For comparison, CT26 tumor tissues from untreated and indo-treated mice were collected for PGE2 measurement at the same time as A20HA tumor samples. (D) Measurement of indo in A20HA tumor tissues. Selected A20HA tumor tissues were used for indo detection by LC/MS. The results are summarized in the bar graphs shown as mean±SEM of three samples per group. (E) The schema depicts the experimental procedures. Mice with established A20HA tumors received CTX-conditioning followed by adoptive transfer of pre-activated HA-specific CD4$^+$ T cells, and a cohort of mice received additional indo administration. On day 11, tumor tissues were collected and processed into single cell suspensions for analysis. Donor T cells in tumor were identified as CD4$^+$Thy1.1$^+$ cells. Cells were stained with a panel of markers to evaluate the frequency, activation status and functionality of the donor T cells. The results are summarized in bar graphs and shown as mean±SEM of six samples per condition. (F) Frequencies of donor T cells in tumor (left), and fraction of cells exhibiting naïve (CD62L$^+$CD44$^-$), effector memory (CD62L$^-$CD44$^+$), and central memory (CD62L$^+$CD44$^+$) markers within the donor T cell population (right). (G) Levels of T cell activation/exhaustion markers PD1 and Tim3 in donor T cells. (H) Cytokine profile of donor T cells. T cells were stimulated with PMA/ionomycin in the presence of GolgiPlug for 3.5 hours before intracellular cytokine staining for the indicated cytokines. (I) Frequencies of Tregs and MDSCs. The frequencies of Tregs in donor T cell population and endogenous CD4$^+$ T cells were determined by Foxp3 staining. The frequencies of MDSCs in tumor were determined by % CD11b$^+$Gr1$^+$ cells. ns: non-significant. (J) Migration and retention of infused HA-specific CD4$^+$ T cells in tumor. Following the procedures depicted in the schema, luciferase-transduced HA-specific CD4$^+$ T cells were transferred to CTX-conditioned A20HA-bearing mice followed by indo administration to a cohort of mice for 28 consecutive days. BLI was conducted periodically to visualize luciferase-expressing donor CD4$^+$ T cells in vivo. Representative images of mice in each group are shown. Results of intratumoral donor T cell luciferase signal intensity quantified as mean±SEM are summarized in (K). Each symbol in the plot represents one mouse. Statistics: (B, F, G, H, I) Unpaired t-test, (C, D) One-way ANOVA followed by Tukey's multiple comparison test. *P<0.05, ***p<0.001, ****p<0.0001, ns: non-significant. ACT, adoptive cell therapy; ANOVA, analysis of variance;

MCL-1 and BCL2 in A20 cells (online supplemental figure 6A–C), which is consistent with published studies reporting that NSAIDs promote cancer cell apoptosis by downregulating prosurvival molecules.[16]

We asked if the increased expression of DR5, driven by indo, would augment apoptosis in cancer cells when triggered by its ligand. Published studies have reported that plate-coated MD5-1, a DR5 agonist antibody, can induce
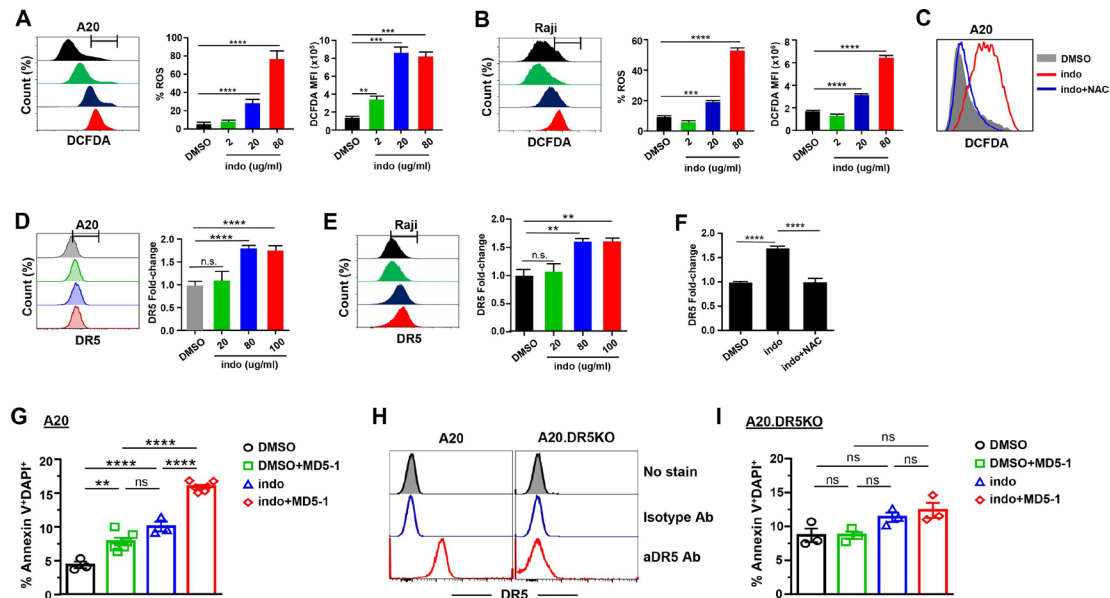
Figure 4 Indomethacin induces ROS and boosts DR5 expression in tumor cells. (A, B) Indo treatment induces ROS in A20 and Raji tumor cells. A20 and Raji cells were cultured overnight in the presence of DMSO or escalating doses of indo. Cells were stained with CM-H2DCFDA to evaluate the ROS levels. Histograms show overlay of CM-H2DCFDA curves. A gate is arbitrarily placed to denote % ROS$^+$ cells. Results of % ROS$^+$ cells under the indicated conditions are summarized in bar graphs and shown as mean±SEM of triplicate samples. The mean fluorescence intensities (MFIs) of CM-H2DCFDA signals are also summarized in bar graphs and shown as mean±SEM of triplicate samples. Data shown are representative of three independent experiments with similar results. (C) The antioxidant NAC reduces ROS production in tumor cells induced by indo. A20 cells were treated with 20 µg/mL indo in the absence or presence of 5 mM NAC overnight before harvesting for CM-H$_2$DCFDA stain. DMSO-treated A20 cells were used as a control. Histograms show overlay of CM-H2DCFDA curves of the indicated samples. (D,E) Indo treatment upregulates DR5 expression in tumor cells. A20 and Raji cells were cultured overnight in the presence of DMSO or indo at the indicated doses. Cells were harvested and stained with anti-DR5 Ab. Histograms show overlay of DR5 curves with a gate arbitrarily placed to denote % DR5$^+$ cells. (F) NAC diminishes DR5 upregulation in indo-treated tumor cells. A20 cells were treated overnight with 80 µg/mL indo in the absence or presence of 5 mM NAC before harvesting for DR5 stain. DMSO-treated A20 cells were used as a control. For samples examined in D–F, the fold-change in % DR5$^+$ cells was calculated using the formula: % DR5$^+$ indo-treated cells/mean of % DR5$^+$ DMSO-treated cells. Results are summarized in bar graphs shown as mean±SEM of triplicate samples for each condition. (G) Indo sensitizes A20 cells to cell death triggered by DR5 signaling. A 96-well protein A-coated plate was coated with PBS or MD5-1 antibody before use. A20 cells were seeded in PBS or MD5-1-coated wells and cultured overnight in the presence of DMSO or indo before harvesting for Annexin V and DAPI staining. Results of % Annexin V$^+$DAPI$^+$ cells are summarized in the bar graph and shown as mean±SEM Each condition contained at least three samples. Results shown are representative of two independent experiments with similar results. (H) Loss of DR5 expression in A20.DR5KO cells. A20.DR5KO cell line was generated by targeted mutagenesis using the CRISPR-Cas9 system. A selected mutant clone was expanded and examined for DR5 expression by flow cytometry. The parental cell line A20 was used for comparison. Unstained cells and isotype antibody-stained cells were included as the controls. (I) A20.DR5KO cells are resistant to cell death induced by MD5-1 or the combination of MD5-1 and indo. A20.DR5KO cells were used to conduct the experiments as described in (A). Results are summarized in the bar graph and shown as mean±SEM of triplicate samples for each condition. Results shown are representative of two independent experiments with similar results. Statistics: (A, B, D–G, I) One-way ANOVA followed by Tukey's multiple comparison test. **P<0.01, ***p<0.001, ****p<0.0001, ns: non-significant. ANOVA, analysis of variance. PBS, phosphate-buffered saline.

DR5 signaling-dependent apoptosis in cultured cells.[34 38] Using this approach, A20 cells were cultured alone, or in the presence of indo and MD5-1 Ab, either alone or in combination. Figure 4G shows that the presence of MD5-1 or indo individually resulted in slight elevation of cell death in A20 cells, whereas the co-presence of MD5-1 and indo led to a more pronounced increase in cell death. To further define the role of DR5 in indo sensitization of A20 cells to MD5-1, we used CRISPR/Cas9 technology to create DR5-deficient A20 cells (A20.DR5KO) (figure 4H). A20.DR5KO cells were unresponsive to MD5-1 (figure 4I, DMSO +MD5-1 vs DMSO), confirming the loss of DR5 signaling in this mutant cell line.

Importantly, indo could no longer sensitize A20.DR5KO cells to MD5-1-induced cell death (figure 4I, indo +MD5-1 vs DMSO +MD5-1 or indo). To confirm that the tumor sensitizing effect of indo was not restricted to A20 cells, we examined the cytotoxicity of indo and activated T cells, either alone or together, on luciferase-expressing 4T1 cells (4T1.Luci) by BLI. We found that the combination of indo and activated T cells exhibited enhanced cytotoxicity to 4T1 cells compared with either treatment alone (online supplemental figure 7). Since the T cells used in the culture were polyclonal, tumor cell killing by T cells was not antigen-driven but likely mediated via ligation of death receptors on tumor cells by their
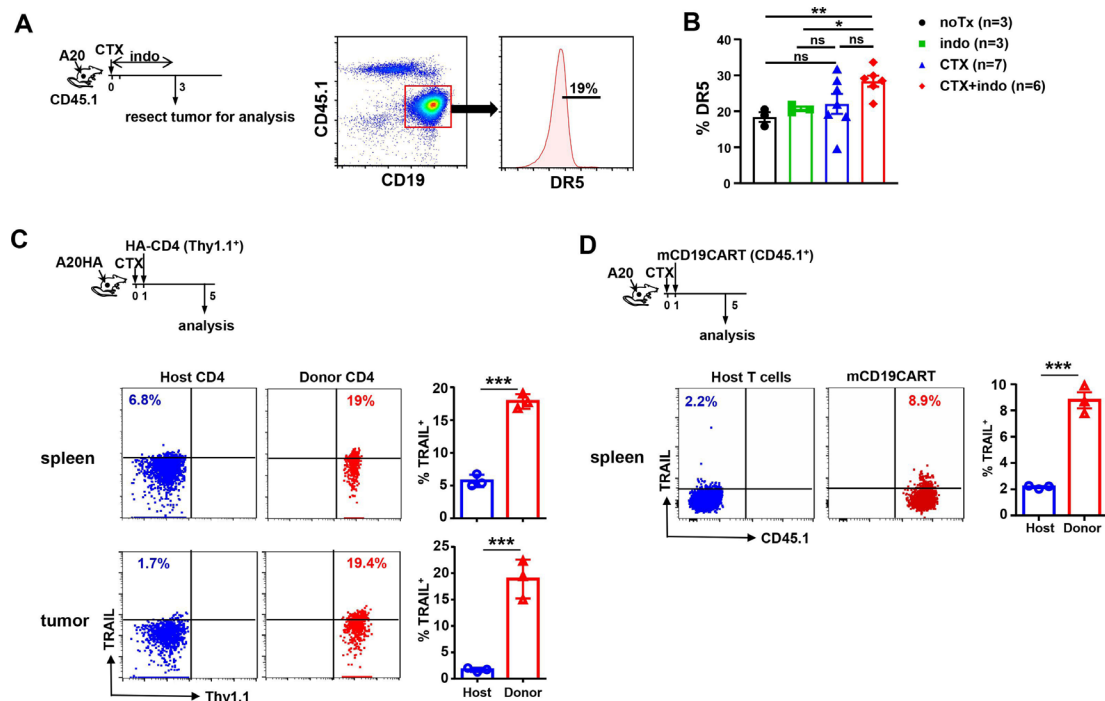
Figure 5 In vivo evidence of increased DR5 expression in tumor cells boosted by indomethacin and upregulation of TRAIL in donor T cells in the ACT setting. (A, B) Indo administration to CTX-treated mice leads to elevated expression of DR5 in tumor cells. Following the experimental procedures depicted in schema, A20 tumor cells (CD45.2[+]) were implanted s.c. to CD45.1 BALB/c mice. Mice with established tumors were divided randomly and received the indicated treatments. Three days after treatment, tumor tissues were resected and processed into single cell suspensions. Gating on live A20 tumor cells (CD45.1^{-} CD19^{+}), the levels of DR5 expression from each sample were evaluated. A gate is arbitrarily placed to denote % DR5^{+} cells. Results of % DR5^{+} cells under the indicated conditions are summarized in the bar graph and shown as mean±SEM Number of mice in each group is given. (C) HA-specific CD4^{+} T cells upregulate TRAIL expression on adoptive transfer. The schema depicts the experimental procedures. Mice with established A20HA tumors received CTX-conditioning followed by adoptive transfer of splenocytes derived from 6.5-Tg mice as described in figure 1A. Four days after T cell transfer, spleen and tumor samples were collected for analysis. Representative dot plots are gated on CD4^{+} cells with numbers denoting percent of TRAIL^{+} cells in donor CD4^{+} T cells (Thy1.1^{+}) and endogenous CD4^{+} T cells (Thy1.1^{-}). Results are summarized in bar graphs and shown as mean±SEM of three samples per group. (D) mCD19CAR T cells upregulate TRAIL expression on adoptive transfer. Following the timeline depicted in the schema, BALB/c mice with established A20 tumors received CTX-conditioning followed by infusion of mCD19CAR T cells (CD45.1^{+}). Four days after T cell infusion, spleen and tumor samples were harvested for analysis. Representative dot plots are gated on CD4^{+} cells with numbers denoting percent of TRAIL^{+} cells in mCD19CAR T cells (CD45.1^{+}) and endogenous CD4^{+} T cells (CD45.1^{-}). Results are summarized in bar graphs and shown as mean±SEM of three samples per group. Data from tumor samples are not shown because the numbers of T cells found in tumors were insufficient to yield reliable results. Statistics: (B) One-way ANOVA followed by Tukey's multiple comparison test, (C, D) Unpaired t-test. *P<0.05, **p<0.01, ***p<0.001, ns: non-significant. ANOVA, analysis of variance.

ligands on T cells. An enhanced engagement of DR5 and its ligand TRAIL between 4T1 cells and activated T cells may account for the improved cytotoxicity when indo and activated T cells were used together. Taken together, our results suggest that the increased expression of DR5, driven by the pro-oxidant activity of indo, can render cancer cells more susceptible to DR5 ligation-induced cell death.

In vivo evidence of indo-boosted DR5 expression in tumor cells and upregulation of TRAIL in donor T cells in the ACT setting

Based on our in vitro data, we posited that indo administration may boost DR5 expression in tumor cells, thereby sensitizing them to T cell cytotoxicity in the ACT setting. We first examined whether indo administration led to DR5 upregulation in tumor cells in vivo. For this purpose, A20 cells were implanted subcutaneously to CD45.1 mice

so that A20 lymphoma cells (CD19^{+}CD45.2^{+}) could be unequivocally distinguished from the endogenous B cells (CD19^{+}CD45.2^{-}) at the time of FACS analysis. Tumor-bearing mice were subjected to four different treatment conditions and tumors were resected for FACS analysis 3 days after treatment (figure 5A). Figure 5B shows that A20 tumor cells recovered from CTX-conditioned, indo-administered mice had significantly increased DR5 expression compared with tumor cells from untreated or indo-treated mice, while DR5 expression in tumor cells from CTX-conditioned mice varied. The data show that indo administration following CTX-preconditioning consistently upregulates DR5 expression in tumor cells. Next, we examined whether the donor T cells were a source of TRAIL. To this end, HA-CD4[act] T cells were transferred to CTX-conditioned A20HA tumor-bearing
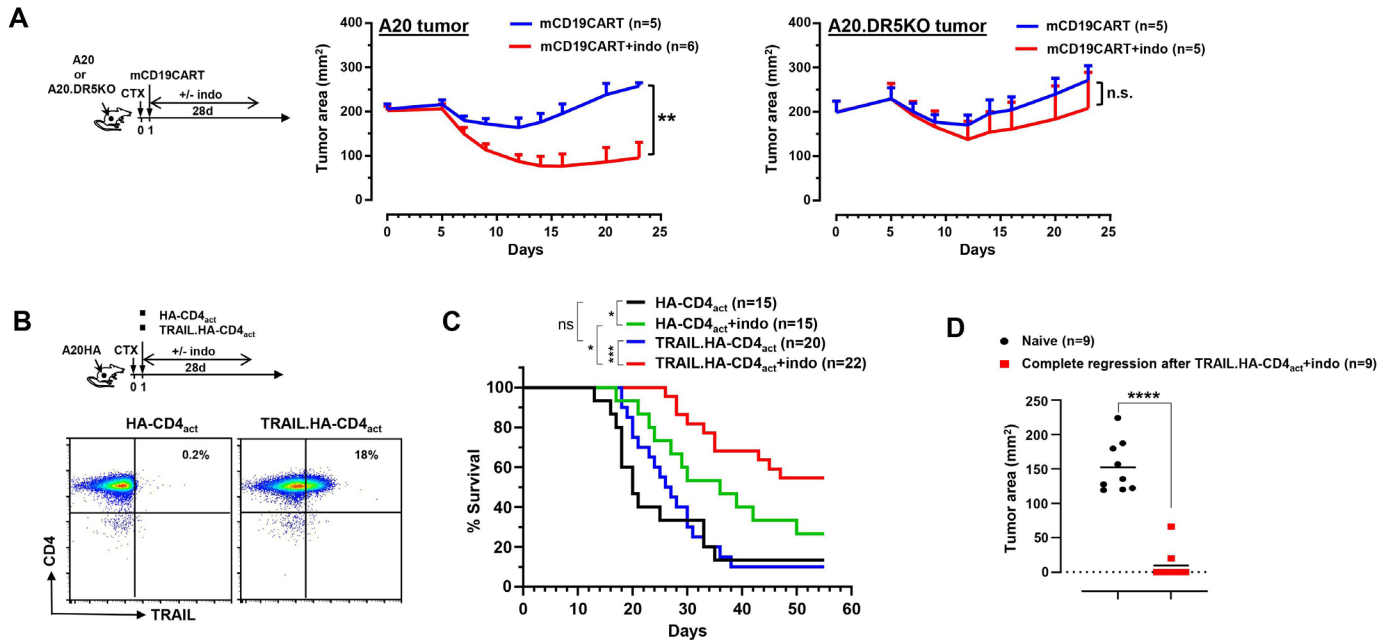
Figure 6 The beneficial effect of indomethacin is dependent on tumor expression of DR5 and can be amplified by TRAIL-overexpressing donor T cells. (A) The beneficial effect of indo in ACT is diminished when tumor cells are DR5-deficient. The schema depicts the experimental procedures. Mice were implanted s.c. with A20 or A20.DR5KO tumor cells. Mice with established tumors (~180 mm²) received CTX-conditioning followed by infusion of mCD19CAR T cells. Half of the mice received daily indo administration for 28 days. Tumor growth curves of each group are shown. Results are presented as mean±SEM of tumor area. Numbers of mice for each group are given. Data shown are representative of two independent experiments with similar results. (B) Preparation of TRAIL-overexpressing T cells for ACT. HA-specific CD4⁺ T cells were transduced with retrovirus to overexpress TRAIL. Expression of TRAIL in transduced T cells was confirmed by flow cytometry. Mock-transduced T cells were used as a control. Following the experimental procedures depicted in the schema, mock or TRAIL-transduced HA-specific CD4⁺ T cells were transferred into CTX-conditioned A20HA-bearing mice. Half of the mice received daily indo administration for 28 days. Tumor growth was monitored by caliper measurement. Results of mouse survival are shown in the Kaplan-Meier plot. (C). Data shown are pooled results from three independent experiments. (D) Mice with complete tumor regression are resistant to tumor rechallenge. Mice that had undergone complete tumor regression after receiving CTX+TRAIL.HA-CD4_act+indo were rechallenged with A20HA tumor cells. Naïve mice injected s.c. with A20HA tumor cells were used as the control. Numbers of mice in each group are given. Statistics: (A, D) Unpaired t-test, (C) Log-rank (Mantel-Cox) test. *P<0.05, **p<0.01, ***p<0.001, ****p<0.0001, ns: non-significant. ACT, adoptive cell therapy.

mice. Five days later, spleens and tumors were collected to examine the levels of TRAIL in the donor CD4⁺ T cells as well as the endogenous CD4⁺ T cells by FACS. Figure 5C shows that TRAIL expression was significantly higher in tumor-specific donor CD4⁺ T cells than in bystander host CD4⁺ T cells. Similar results were obtained in the mCD19CART model in which mCD19CART cells exhibited higher TRAIL expression than endogenous T cells (figure 5D). These in vivo data support the possibility that indo administration enables enhanced TRAIL-DR5 engagement between donor T cells and tumor cells in the ACT setting.

The beneficial effect of indo is dependent on tumor cell DR5 expression and can be amplified by TRAIL overexpression in donor T cells

We postulated that if the beneficial effect of indo in ACT is due to enhanced TRAIL-DR5 engagement, then DR5-deficiency in tumor cells would nullify this effect. To test this, mice inoculated with A20 or A20.DR5KO tumor cells were treated with CTX followed by mCD19CAR T cell transfer, in the absence or presence of indo administration

(figure 6A schema). Confirming our prior observation (figure 2D,E), indo administration significantly improved the effectiveness of mCD19CART in controlling the growth of A20 tumors (figure 6A, left graph). In contrast, the beneficial effect of indo on mCD19CART was abolished in mice bearing A20.DR5KO tumors (figure 6A, right graph). It is worth noting that A20 and A20.DR5KO tumors exhibited similar growth kinetics in response to mCD19CART in the absence of indo, indicating that the basal level of DR5 in A20 tumor cells, even if ligated by TRAIL from the CAR T cells, is insufficient to cause tumor cell death to an extent that confers discernable therapeutic benefit. In addition, A20.DR5KO and A20 tumors grew at similar rates in untreated mice (data not shown), suggesting that DR5 deficiency per se does not alter tumor growth kinetics in mice. Together, these data indicate that the beneficial effect of indo in the context of ACT relies on tumor cell DR5 expression.

We reasoned that enhancing TRAIL expression in donor T cells may lead to more effective engagement with indo-boosted DR5 in tumor cells to intensify tumor

cell apoptosis, resulting in further improvement in therapeutic outcomes. To test this, HA-CD4$_{act}$ T cells were virally transduced to overexpress TRAIL (TRAIL.HA-CD4$_{act}$) at the time of transfer (figure 6B). Notably, indo administration following TRAIL.HA-CD4$_{act}$ T cell transfer exhibited markedly improved survival benefit, with over 50% of mice achieving complete tumor regression compared with less than 30% complete tumor regression in mice that received HA-CD4$_{act}$ and indo (figure 6C). Interestingly, TRAIL.HA-CD4$_{act}$ T cell transfer in the absence of indo did not result in improvement of mouse survival compared with HA-CD4$_{act}$ T cell transfer, indicating that the enhanced expression of DR5, boosted by indo, is essential for sensitizing cancer cells to TRAIL-expressing T cells. Mice showing complete tumor regression after receiving the TRAIL.HA-CD4$_{act}$ and indo combination treatment were rechallenged with A20HA tumor cells. Seven out of nine mice were completely protected from tumor growth, and the remaining two mice had significantly lower tumor burden compared with tumor-challenged naïve mice, indicating the development of immune memory (figure 6D).

DISCUSSION

Here, we demonstrate that indo administration can augment the efficacy of ACT against mouse and human B-cell lymphomas using T cells expressing a tumor-specific TCR or CD19CAR. Mechanistically, our data reveal that the ability of indo to potentiate ACT relies on its pro-oxidative activity that leads to enhanced engagement of the TRAIL-DR5 axis between tumor-reactive T cells and tumor cells. To our knowledge, our study provides the first in vivo evidence that the use of NSAID such as indo is compatible with and can benefit T cell-based adoptive immunotherapy.

Multiple lines of evidence have documented that the antitumor activity of NSAIDs can be multifaceted, likely involving inhibition of COX and blockage of PGE2 synthesis, as well as other COX-independent mechanisms, such as suppression of Wnt/β-catenin signaling, downregulation of survival molecules, induction of oxidative/ER stress, and fostering an immunogenic milieu in the TME. As an inflammatory mediator, PGE2 is known to promote tumor progression, metastasis, angiogenesis and chemoresistance.[23 36] PGE2 can induce Treg cells and MDSCs, thereby exerting potent immunosuppression on tumor-reactive T cells and NK cells.[23 24] PGE2 can be produced by tumor cells as well as stromal cells, such as myeloid cells and fibroblasts.[39 40] It has been shown in various mouse tumor models that inhibition of COX2 or PGE2 can mitigate immunosuppression and promote antitumor immunity.[23 24] Suppression of COX/PGE2 is well-established to be the major mechanism by which NSAIDs, such as celecoxib and aspirin, enhance the efficacy of anti-PD-1 therapy in multiple mouse tumor models.[25 26]

Here, we show that A20 tumor cells barely express COX2 and produce a negligible amount of PGE2. Moreover, PGE2 was not detected in the tumor masses resected from mice implanted with A20HA tumors. Our in vivo studies show that indo administration alone marginally altered tumor growth and mouse survival compared with untreated mice in the A20HA (figure 1B,C) and A20 (figure 2E) models. We also did not detect PGE2 in human B-cell lymphoma Raji cell culture (data not shown), consistent with the results of a previous report showing that human B-cell lymphoma cells do not produce PGE2.[39] In accordance with what we observed in the murine lymphoma model, indo administration alone did not delay Raji growth in NSG mice, nor did it improve mouse survival (figure 2F,G). These results indicate that the COX/PGE2 axis does not contribute to tumor progression in the B-cell lymphoma models used in our study. Therefore, the beneficial effect of indo in ACT is unlikely attributable to COX inhibition and PGE2 reduction. The COX-independent ACT-potentiating effect of indo may have important implications for repurposing and expanding the use of NSAIDs in cancer immunotherapy. A variety of other NSAIDs besides indo can be tested to identify those that are most effective and least toxic in the setting of ACT. In addition, novel non-COX inhibitory derivatives of NSAIDs can be developed to suit the needs of ACT while reducing the potential adverse effects associated with COX inhibition, such as gastrointestinal, renal, and cardiovascular toxicities.[41]

Although our study underscores the importance of the TRAIL-DR5 axis in indo-mediated enhancement of ACT efficacy, our results do not exclude other mechanisms by which indo may contribute to an improved therapeutic outcome. It is conceivable that for tumors with high levels of COX/PGE2, indo administration can inhibit this pro-tumorigenic signaling pathway and thus exert direct antitumor effects. Meanwhile, indo may mitigate PGE2-driven immunosuppression in the TME, thereby conditioning a favorable immune milieu for ACT. Moreover, indo-mediated downregulation of prosurvival molecules, including c-FLIP, MCL-1, BCL2 and survivin may further promote tumor eradication. These distinct but mutually reinforcing mechanisms may synergize with ACT to achieve substantially improved therapeutic outcomes, even for hard-to-treat solid tumors, which often express high levels of COX/PGE2.

The initial finding that ligation of death receptors (DR4 and DR5) by their ligand TRAIL leads to selective death in cancer cells incentivized the development of recombinant human TRAIL (rhTRAIL) and death receptor agonist antibodies as cancer therapeutics. Despite the promising data from numerous preclinical studies, results from clinical studies showed limited efficacy of these reagents as monotherapy.[42–47] The TRAIL or death receptor-based therapies have limitations related to the short half-life of rhTRAIL, heterogeneous expression of death receptors in cancer, weak agonistic potential of anti-DR4 or anti-DR5 antibodies, and acquisition of resistance by cancer cells. There is emerging evidence that engagement of the TRAIL-DR5 axis can be attained through cellular therapy

to drive a robust antitumor effect. It has been shown that mice reconstituted with TRAIL-transduced bone marrow cells were less prone to tumor growth following engraftment.[48] Using a murine model of allogeneic hematopoietic stem cell transplantation, Ghosh *et al* reported that infusion of TRAIL-overexpressing T cells can achieve a curative result in tumor-bearing mice by increasing graft-versus-tumor response while suppressing graft-versus-host disease.[49] With direct relevance to adoptive T cell therapy using CAR T cells, DeSelm *et al* reported that TRAIL produced by CAR T cells on recognizing the targeted antigen on tumor cells can eliminate antigen-negative tumor cells previously exposed to low-dose radiation.[50] Moreover, two recent CRISPR-based screening studies demonstrated that tumor-intrinsic death receptor signaling critically regulates CD19CAR T cell cytotoxicity and functional exhaustion.[51 52] Based on these published studies and our current data, we put forth the hypothesis that simultaneous upregulation of TRAIL in donor T cells and DR5 in cancer cells can further magnify cell death in cancer cells. Our data suggest that ectopic expression of TRAIL on the surface of donor T cells has the advantage of providing a reliable source of TRAIL to effectively crosslink DR5 in a localized manner. Overexpression of TRAIL in tumor-specific T cells, especially those engineered to express CARs or TCRs, can be readily achieved during the T cell genetic modification process.

One potential concern for enhancing TRAIL-DR5 engagement in the ACT setting is whether fratricide will occur among donor T cells. Although others have shown that activated T cells, including CAR T cells, are prone to DR5-mediated cell death,[53 54] we did not observe any obvious detrimental effects on donor T cells when mice received indo treatment or when donor T cells were genetically modified to overexpress TRAIL. The exact mechanism of the differential response of tumor cells and donor T cells to indomethacin is not clear. It is possible that cancer cells are more sensitive than T cells to indomethacin at a certain dose range because cancer cells are known to have higher basal levels of endogenous oxidative stress as compared with normal cells.[6] From a practical perspective, if TRAIL-induced apoptosis in T cells does become a concern, this issue can be addressed by engineering T cells to overexpress a dominant negative form of DR5 to disrupt DR5 signaling, or an antioxidant gene such as catalase to mitigate oxidative stress. In this regard, it has been reported that T cells engineered to coexpress CAR and catalase exhibit potent antitumor activity.[55]

In summary, our study demonstrates that the pro-oxidative property of indo can be exploited to enhance death receptor signaling in cancer cells, providing rationale for combining indo with genetically modified T cells to intensify tumor cell killing through the TRAIL-DR5 axis. These findings implicate indo administration, and potentially similar use of other NSAIDs, as a readily applicable and cost-effective approach to augment the efficacy of ACT.

Author affiliations
[1]Georgia Cancer Center, Augusta University, Augusta, Georgia, USA
[2]Division of Biostatistics & Data Science, Department of Population Health Sciences, Medical College of Georgia, Augusta University, Augusta, Georgia, USA
[3]McWhorter School of Pharmacy, Samford University, Birmingham, Alabama, USA
[4]Department of Pathology, Medical College of Georgia, Augusta University, Augusta, Georgia, USA
[5]Blood and Marrow Transplant & Cellular Immunotherapy Department, H Lee Moffitt Cancer Center and Research Institute, Tampa, Florida, USA
[6]Department of Medicine, Medical College of Georgia, Augusta University, Augusta, Georgia, USA
[7]Department of Pediatrics, Medical College of Georgia, Augusta University, Augusta, Georgia, USA
[8]Drug Discovery and Development, Harrison School of Pharmacy, Auburn University, Auburn, Alabama, USA

ORCID iDs
Nada S Aboelella http://orcid.org/0000-0002-9009-9897
Gregory Gorman http://orcid.org/0000-0003-4306-8884
Marco L Davila http://orcid.org/0000-0002-6270-3065
Gang Zhou http://orcid.org/0000-0001-8967-114X

REFERENCES
1 Guedan S, Ruella M, June CH. Emerging cellular therapies for cancer. *Annu Rev Immunol* 2019;37:145–71.
2 Weber EW, Maus MV, Mackall CL. The emerging landscape of immune cell therapies. *Cell* 2020;181:46–62.

3 Magalhaes I, Carvalho-Queiroz C, Hartana CA, *et al*. Facing the future: challenges and opportunities in adoptive T cell therapy in cancer. *Expert Opin Biol Ther* 2019;19:811–27.

4 Hong M, Clubb JD, Chen YY. Engineering CAR-T cells for next-generation cancer therapy. *Cancer Cell* 2020;38:473–88.

5 Majzner RG, Mackall CL. Clinical lessons learned from the first leg of the CAR T cell journey. *Nat Med* 2019;25:1341–55.

6 Storz P. Reactive oxygen species in tumor progression. *Front Biosci* 2005;10:1881–96.

7 Aboelella NS, Brandle C, Kim T, *et al*. Oxidative stress in the tumor microenvironment and its relevance to cancer immunotherapy. *Cancers* 2021;13:986. doi:10.3390/cancers13050986

8 Trachootham D, Alexandre J, Huang P. Targeting cancer cells by ROS-mediated mechanisms: a radical therapeutic approach? *Nat Rev Drug Discov* 2009;8:579–91.

9 Gorrini C, Harris IS, Mak TW. Modulation of oxidative stress as an anticancer strategy. *Nat Rev Drug Discov* 2013;12:931–47.

10 Nogueira V, Hay N. Molecular pathways: reactive oxygen species homeostasis in cancer cells and implications for cancer therapy. *Clin Cancer Res* 2013;19:4309–14.

11 Wang J, Yi J. Cancer cell killing via ROS: to increase or decrease, that is the question. *Cancer Biol Ther* 2008;7:1875–84.

12 Schumacker PT. Reactive oxygen species in cancer cells: live by the sword, die by the sword. *Cancer Cell* 2006;10:175–6.

13 Habtetsion T, Ding Z-C, Pi W, *et al*. Alteration of tumor metabolism by CD4+ T cells leads to TNF-α-dependent intensification of oxidative stress and tumor cell death. *Cell Metab* 2018;28:228–42.

14 Tsutsumi S, Gotoh T, Tomisato W, *et al*. Endoplasmic reticulum stress response is involved in nonsteroidal anti-inflammatory drug-induced apoptosis. *Cell Death Differ* 2004;11:1009–16.

15 Adachi M, Sakamoto H, Kawamura R, *et al*. Nonsteroidal anti-inflammatory drugs and oxidative stress in cancer cells. *Histol Histopathol* 2007;22:437–42.

16 Ralph SJ, Pritchard R, Rodríguez-Enríquez S, *et al*. Hitting the bull's-eye in metastatic cancers-NSAIDs elevate ROS in mitochondria, inducing malignant cell death. *Pharmaceuticals* 2015;8:62–106.

17 Cha W, Park S-W, Kwon T-K, *et al*. Endoplasmic reticulum stress response as a possible mechanism of cyclooxygenase-2-independent anticancer effect of celecoxib. *Anticancer Res* 2014;34:1731–5.

18 Marchetti M, Resnick L, Gamliel E, *et al*. Sulindac enhances the killing of cancer cells exposed to oxidative stress. *PLoS One* 2009;4:e5804.

19 Raza H, John A, Benedict S. Acetylsalicylic acid-induced oxidative stress, cell cycle arrest, apoptosis and mitochondrial dysfunction in human hepatoma HepG2 cells. *Eur J Pharmacol* 2011;668:15–24.

20 Tse AK-W, Cao H-H, Cheng C-Y, *et al*. Indomethacin sensitizes TRAIL-resistant melanoma cells to TRAIL-induced apoptosis through ROS-mediated upregulation of death receptor 5 and downregulation of survivin. *J Invest Dermatol* 2014;134:1397–407.

21 Pritchard R, Rodríguez-Enríquez S, Pacheco-Velázquez SC, *et al*. Celecoxib inhibits mitochondrial O_2 consumption, promoting ROS dependent death of murine and human metastatic cancer cells via the apoptotic signalling pathway. *Biochem Pharmacol* 2018;154:318–34.

22 Ralph SJ, Nozuhur S, Moreno-Snchez R, *et al*. NSAID celecoxib: a potent mitochondrial pro-oxidant cytotoxic agent sensitizing metastatic cancers and cancer stem cells to chemotherapy. *J Cancer Metastasis Treat* 2018;4:49.

23 Finetti F, Travelli C, Ercoli J, *et al*. Prostaglandin E2 and cancer: insight into tumor progression and immunity. *Biology* 2020;9:9120434. doi:10.3390/biology9120434

24 Hussain M, Javeed A, Ashraf M, *et al*. Non-steroidal anti-inflammatory drugs, tumour immunity and immunotherapy. *Pharmacol Res* 2012;66:7–18.

25 Zelenay S, van der Veen AG, Böttcher JP, *et al*. Cyclooxygenase-dependent tumor growth through evasion of immunity. *Cell* 2015;162:1257–70.

26 Pelly VS, Moeini A, Roelofsen LM, *et al*. Anti-inflammatory drugs remodel the tumor immune environment to enhance immune checkpoint blockade efficacy. *Cancer Discov* 2021;11:2602–19.

27 Torres-Collado A, Jazirehi A. Overcoming resistance of human non-hodgkin's lymphoma to CD19-CAR CTL therapy by celecoxib and histone deacetylase inhibitors. *Cancers* 2018;10:200.

28 Ding Z-C, Huang L, Blazar BR, *et al*. Polyfunctional CD4+ T cells are essential for eradicating advanced B-cell lymphoma after chemotherapy. *Blood* 2012;120:2229–39.

29 Ding Z-C, Blazar BR, Mellor AL, *et al*. Chemotherapy rescues tumor-driven aberrant CD4+ T-cell differentiation and restores an activated polyfunctional helper phenotype. *Blood* 2010;115:2397–406.

30 Kochenderfer JN, Yu Z, Frasheri D, *et al*. Adoptive transfer of syngeneic T cells transduced with a chimeric antigen receptor that recognizes murine CD19 can eradicate lymphoma and normal B cells. *Blood* 2010;116:3875–86.

31 Ding Z-C, Liu C, Cao Y, *et al*. IL-7 signaling imparts polyfunctionality and stemness potential to CD4(+) T cells. *Oncoimmunology* 2016;5:e1171445.

32 Boucher JC, Li G, Kotani H, *et al*. CD28 costimulatory domain-targeted mutations enhance chimeric antigen receptor T-cell function. *Cancer Immunol Res* 2021;9:62–74.

33 Zheng Z, Chinnasamy N, Morgan RA. Protein L: a novel reagent for the detection of chimeric antigen receptor (CAR) expression by flow cytometry. *J Transl Med* 2012;10:29.

34 Stagg J, Sharkey J, Pommey S, *et al*. Antibodies targeted to TRAIL receptor-2 and ErbB-2 synergize in vivo and induce an antitumor immune response. *Proc Natl Acad Sci U S A* 2008;105:16254–9.

35 Ding Z-C, Shi H, Aboelella NS, *et al*. Persistent STAT5 activation reprograms the epigenetic landscape in CD4+ T cells to drive polyfunctionality and antitumor immunity. *Sci Immunol* 2020;5:5962. doi:10.1126/sciimmunol.aba5962

36 Wang D, Dubois RN. Eicosanoids and cancer. *Nat Rev Cancer* 2010;10:181–93.

37 Xu L, Stevens J, Hilton MB, *et al*. COX-2 inhibition potentiates antiangiogenic cancer therapy and prevents metastasis in preclinical models. *Sci Transl Med* 2014;6:242ra84.

38 Frew AJ, Lindemann RK, Martin BP, *et al*. Combination therapy of established cancer using a histone deacetylase inhibitor and a TRAIL receptor agonist. *Proc Natl Acad Sci U S A* 2008;105:11317–22.

39 Gallouet A-S, Travert M, Bresson-Bepoldin L, *et al*. COX-2-independent effects of celecoxib sensitize lymphoma B cells to TRAIL-mediated apoptosis. *Clin Cancer Res* 2014;20:2663–73.

40 Yu M, Guo G, Zhang X, *et al*. Fibroblastic reticular cells of the lymphoid tissues modulate T cell activation threshold during homeostasis via hyperactive cyclooxygenase-$_2$/prostaglandin E_2 axis. *Sci Rep* 2017;7:3350.

41 Piazza GA, Ward A, Chen X, *et al*. PDE5 and PDE10 inhibition activates cGMP/PKG signaling to block Wnt/β-catenin transcription, cancer cell growth, and tumor immunity. *Drug Discov Today* 2020;25:1521–7.

42 Micheau O, Shirley S, Dufour F. Death receptors as targets in cancer. *Br J Pharmacol* 2013;169:1723–44.

43 Lemke J, von Karstedt S, Zinngrebe J, *et al*. Getting TRAIL back on track for cancer therapy. *Cell Death Differ* 2014;21:1350–64.

44 de Miguel D, Lemke J, Anel A, *et al*. Onto better TRAILs for cancer treatment. *Cell Death Differ* 2016;23:733–47.

45 Yuan X, Gajan A, Chu Q, *et al*. Developing TRAIL/TRAIL death receptor-based cancer therapies. *Cancer Metastasis Rev* 2018;37:733–48.

46 Wajant H. Molecular mode of action of TRAIL receptor agonists-common principles and their translational exploitation. *Cancers* 2019;11:11070954. doi:10.3390/cancers11070954

47 Snajdauf M, Havlova K, Vachtenheim J, *et al*. The TRAIL in the treatment of human cancer: an update on clinical trials. *Front Mol Biosci* 2021;8:628332.

48 Song K, Benhaga N, Anderson RL, *et al*. Transduction of tumor necrosis factor-related apoptosis-inducing ligand into hematopoietic cells leads to inhibition of syngeneic tumor growth in vivo. *Cancer Res* 2006;66:6304–11.

49 Ghosh A, Dogan Y, Moroz M, *et al*. Adoptively transferred TRAIL+ T cells suppress GVHD and augment antitumor activity. *J Clin Invest* 2013;123:2654–62.

50 DeSelm C, Palomba ML, Yahalom J, *et al*. Low-dose radiation conditioning enables CAR T cells to mitigate antigen escape. *Mol Ther* 2018;26:2542–52.

51 Dufva O, Koski J, Maliniemi P, *et al*. Integrated drug profiling and CRISPR screening identify essential pathways for CAR T-cell cytotoxicity. *Blood* 2020;135:597–609.

52 Singh N, Lee YG, Shestova O, *et al*. Impaired death receptor signaling in leukemia causes antigen-independent resistance by inducing CAR T-cell dysfunction. *Cancer Discov* 2020;10:552–67.

53 Janssen EM, Droin NM, Lemmens EE, *et al*. CD4+ T-cell help controls CD8+ T-cell memory via TRAIL-mediated activation-induced cell death. *Nature* 2005;434:88–93.

54 Tschumi BO, Dumauthioz N, Marti B, *et al*. Correction to: CART cells are prone to Fas- and DR5-mediated cell death. *J Immunother Cancer* 2018;6:92.

55 Ligtenberg MA, Mougiakakos D, Mukhopadhyay M, *et al*. Coexpressed catalase protects chimeric antigen Receptor-Redirected T cells as well as bystander cells from oxidative stress-induced loss of antitumor activity. *J Immunol* 2016;196:759–66.